Characterization of Diamond like carbon coating on polished stainless steel plate from University of West of Scotland

V.Bavigadda, A.Chiummo, R.Day, A.Magazzu, G.Pillant

EGO - European Gravitational Observatory

Table of Contents

1. Introduction

In this document we report about the characterization of Diamond-Like Carbon (DLC) for application in gravitational-wave interferometric antennas as beam-dump of laser power at wavelength λ =1.064um (Nd:YAG laser) [1,2]. A similar work was previously carried out by Takahashi [3], in the framework of the now decommissioned Japanese interferometric antenna TAMA300. Taking advantage of their early results, we decided to test DLC coatings on stainless steel 304 (X5CrNi18-10). The resulting layer is *micro-conformal*, i.e. it reproduces the same micro-roughness as the substrate. Of course this shifts the roughness requirements on the substrate surface.

The tests we performed within the scope of the present work have been done upon some samples coated by Thin-Film Centre – University of West Scotland. In this document, we summarize the related tests performed for three different DLC coated samples. We have measured the total integrated scattering (TIS), the reflectivity, the refractive index and the damage threshold under vacuum for the DLC coating.

2. Sample description

The characterized samples consist of a substrate and DLC coating layer. The substrates are made of mirror polished stainless steel plates with dimensions 50mm×50mm×2mm. The DLC layers of thickness ≈1.91, 9.76, 19.8um were deposited by the manufacturer at University of West of Scotland. The thickness of DLC layers were measured on silicon substrates, so there may be very slight difference in thickness values for DLC layers coated on stainless steel substrates.

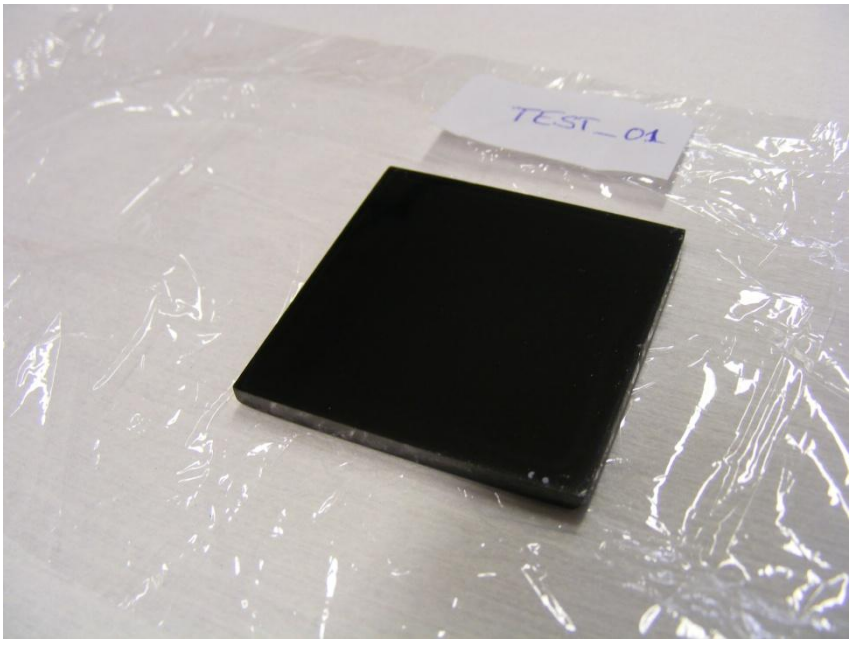

Figure 1: A sample with DLC coating on a polished stainless steel substrate

3. Reflectivity, Refractive index and Absorption

To characterize the optical behavior of the DLC coating, we have performed several measurements of reflectivity for test samples. By measuring the reflectivity as a function of the angle of incidence, we can determine the complex index of refraction and hence the Fresnel reflectivity and the absorption of the material. Due to the electromagnetic nature of the light propagation, the polarization state (S or P) of the beam needs to be taken into consideration to derive the reflectivity.

The following expressions are derived for reflectivity based on the figure 1. We assume three different dielectric media with different indices of refraction n_0, n_1 and n_2. The top surface has refractive index n_0 (air), the bottom surface is the substrate (stainless-steel) has the refractive index n2 and the layer on top of the substrate has refractive index n1 (DLC). The reflectivity is determined using Fresnel's equations.

$$r_{1,s} = \frac{n_0 cos(\theta_0) - n_1 cos(\theta_1)}{n_0 cos(\theta_0) + n_1 cos(\theta_1)} \quad (1)$$

$$r_{1,p} = \frac{n_0 cos(\theta_1) - n_1 cos(\theta_0)}{n_0 cos(\theta_1) + n_1 cos(\theta_0)} \quad (2)$$

$$r_{2,s} = \frac{n_1 cos(\theta_1) - n_2 cos(\theta_2)}{n_1 cos(\theta_1) + n_2 cos(\theta_2)} \quad (3)$$

$$r_{2,p} = \frac{n_1 cos(\theta_2) - n_2 cos(\theta_1)}{n_1 cos(\theta_2) + n_2 cos(\theta_1)} \quad (4)$$

where $n_2 sin(\theta_2) = n_1 sin(\theta_1)$; $n_1 sin(\theta_1) = n_0 sin(\theta_0)$

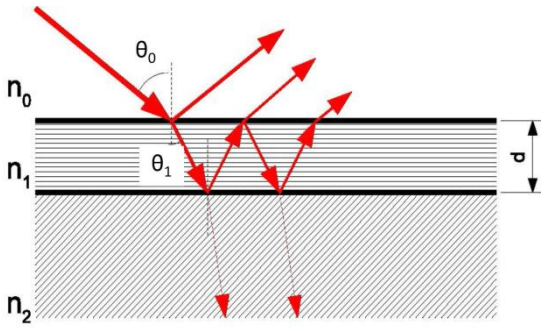

Figure 2: Sketch of the reflection process with two dielectric interfaces at a distance d

The light impinges onto the first dielectric surface from medium with refractive index n_0 at an angle θ_0 is partially reflected and the rest is refracted at an angle θ_1 inside the medium with refractive index n_1. This light reflects again at the second surface whose refractive index is n_2. The fraction of the light that is reflected from second surface crosses again the interface between n_1 and n_0. This light interferes with the light reflected from the first surface. The reflected light from the second surface has a phase lag of

$$2\delta_1 = \frac{4\pi}{\lambda} n_1 d\cos(\theta_1) \tag{5}$$

If the thickness of the film is of the order of one or some wavelengths of the incident light (d ~ 1-10 λ), then the interference between the light reflected from first and second surfaces has to be taken into account. The resulting amplitude reflectivity is given by the Airy's sum of the fields coming from the two interfaces:

$$r_{s,p}(\theta_0) = \frac{r_{1s,p}(\theta_0) + r_{2s,p}(\theta_1) exp(-2i\delta_1)}{1 + r_{1s,p}(\theta_0) r_{2s,p}(\theta_1) exp(-2i\delta_1)} \tag{6}$$

where *r* stands for Fresnel's amplitude reflectivity (with subscripts 1 or 2 according to the interfaces air/DLC or DLC/metal, and s or p according to the polarizations); $\theta_1 = \frac{n_0}{n_1} sin^{-1}(\theta_0)$ is the angle inside the DLC layer (refractive index n_1). Of course, when the index of refraction n1 has a non-negligible imaginary part, as it is the case for DLC, the term $exp(-2i\delta_1)$ describes also absorption inside the medium.

3.1. Reflectivity for P and S polarization

The optical setup for measuring the reflectivity was built with a collimated YAG laser beam (beam size w ~ 0.4mm). The laser beam was expanded using a negative lens (f = 20cm) and a quarter wave plate which linearly polarizes the beam. A pair of half wave plates HWP1; 2 and two polarizing beam splitters PBS1; 2 were used to control the state of polarization (either to set in P or S) and the beam power (high or low). The mirrors M1, M2 and M3 steers the laser beam on to the DLC coated sample at required height from the optical bench. The laser beam after passing through HWP2 was analyzed by a polarizing beam-splitter (PBS3) to ensure that it stays only in a single polarization state (either in P or S). The unwanted light was dumped with beam dumps BD1; 2; 3 and 4. A rotation stage was designed in such a way that the central part where the sample was mounted rotates only a half with respect to the outer edge. A photo-diode (PD) sensor mounted at the outer edge of the rotation stage reads the reflected beam power. Care was taken to align the sample mount so that the reflected light beam stays always on the center part of the PD active area.

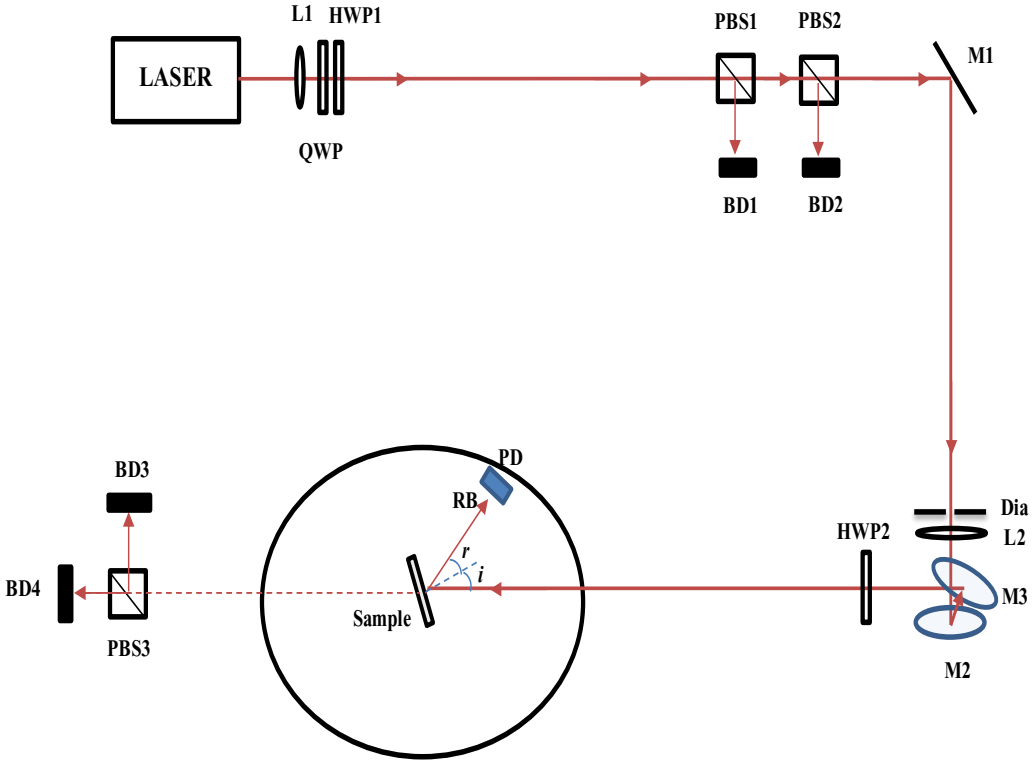

Figure 3 Reflectivity measurement setup

We measured the reflectivity at the YAG laser wavelength (λ = 1064nm) for S and P polarizations for the test samples coated with a 1.91µm, 9.76µm and 19.8µm thick DLC layers (labeled as Test-01, 02 and 03). For the thinner DLC layer (thickness d ~ λ), the reflection of Test-01 has to be modeled by taking into account the reflectivity at the interface between DLC and Stainless Steel as well (see [2,3]). The reflectivity of DLC was determined by fitting the square of the absolute value of the amplitude of reflectivity ($|r^2|$) with the measured data depending on the state of the polarization of the incident beam. The reflectivity of stainless-steel has been determined previously in a similar way by fitting the reflectivity data to the Fresnel's equations (see [2]).

3.2. Index of refraction using local fitting

We have measured the reflectivity for three DLC coated samples with different thickness values; hence the measured data was fitted individually for each of the samples. We call this method as individual curve fitting.

The best fit values for n_1 was found by finding the minimum in the residual between the fitted data and the measured data for that particular sample using 'fminsearch' command in MATLAB. In this process, the equation for estimating the residual was defined as a function of n1 and d. Once the optimum value for n1 found, it was used to plot the theoretically calculated data.

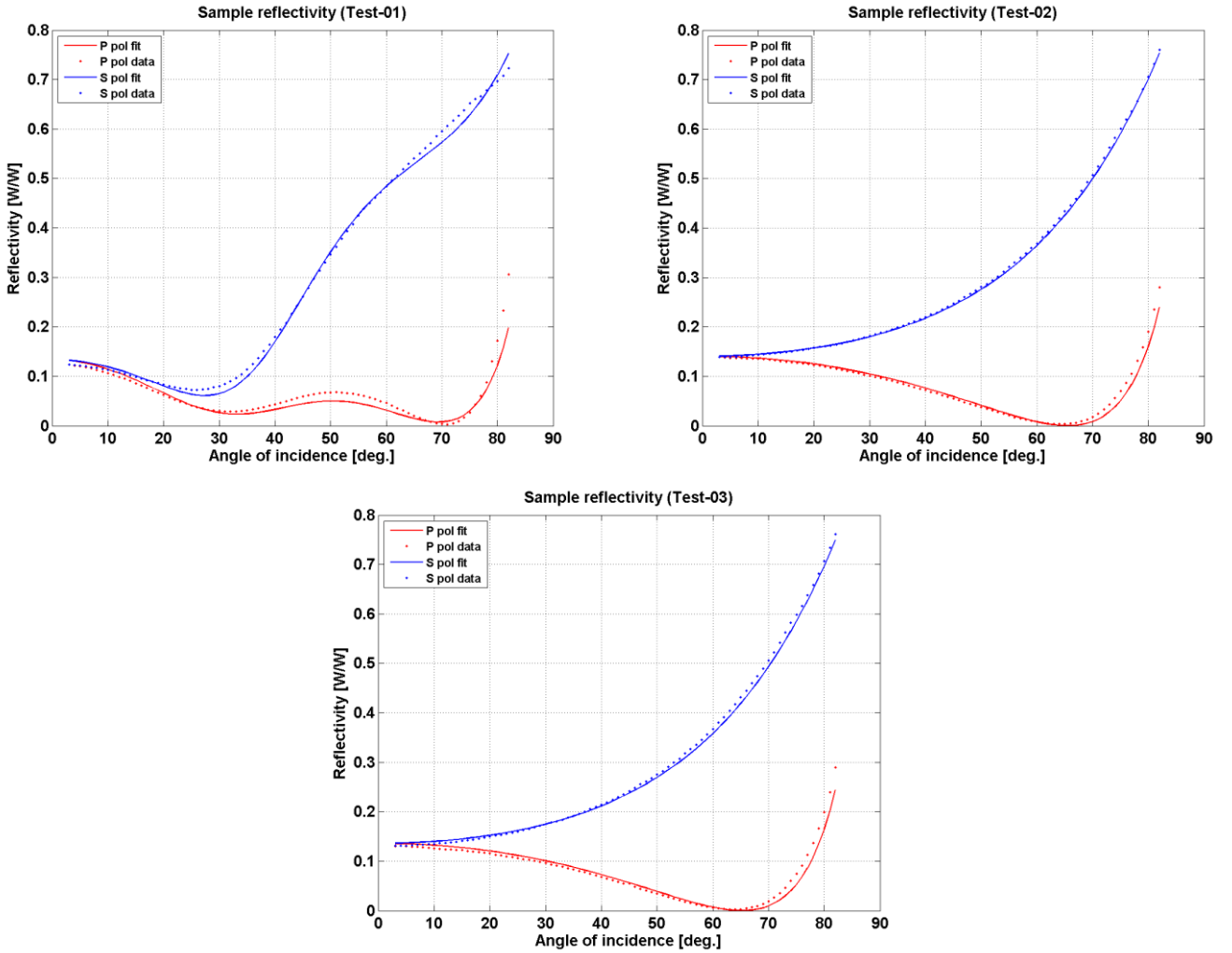

Figure 4: Individual fitting for the DLC coated samples (a) of thickness 1.91µm (b) 9.76µm (c) 19.8µm

where P pol fit: Reflectivity for P-polarized incident beam for local fit;
P pol data: Reflectivity measured for P-polarized incident beam;
S pol fit: Reflectivity for S-polarized incident beam for local fit;
S pol data: Reflectivity measured for S-polarized incident beam;

3.3. Index of refraction using global fitting

The global curve fitting was carried out by determining the minimum residual between theoretically calculated and experimentally obtained reflectivity values for all the samples together. The minimum in global residual was found by summing up the individual residuals corresponding to each of the samples. The optimum value of n_1 was substituted back into the reflectivity equations and plotted the theoretically calculated data.

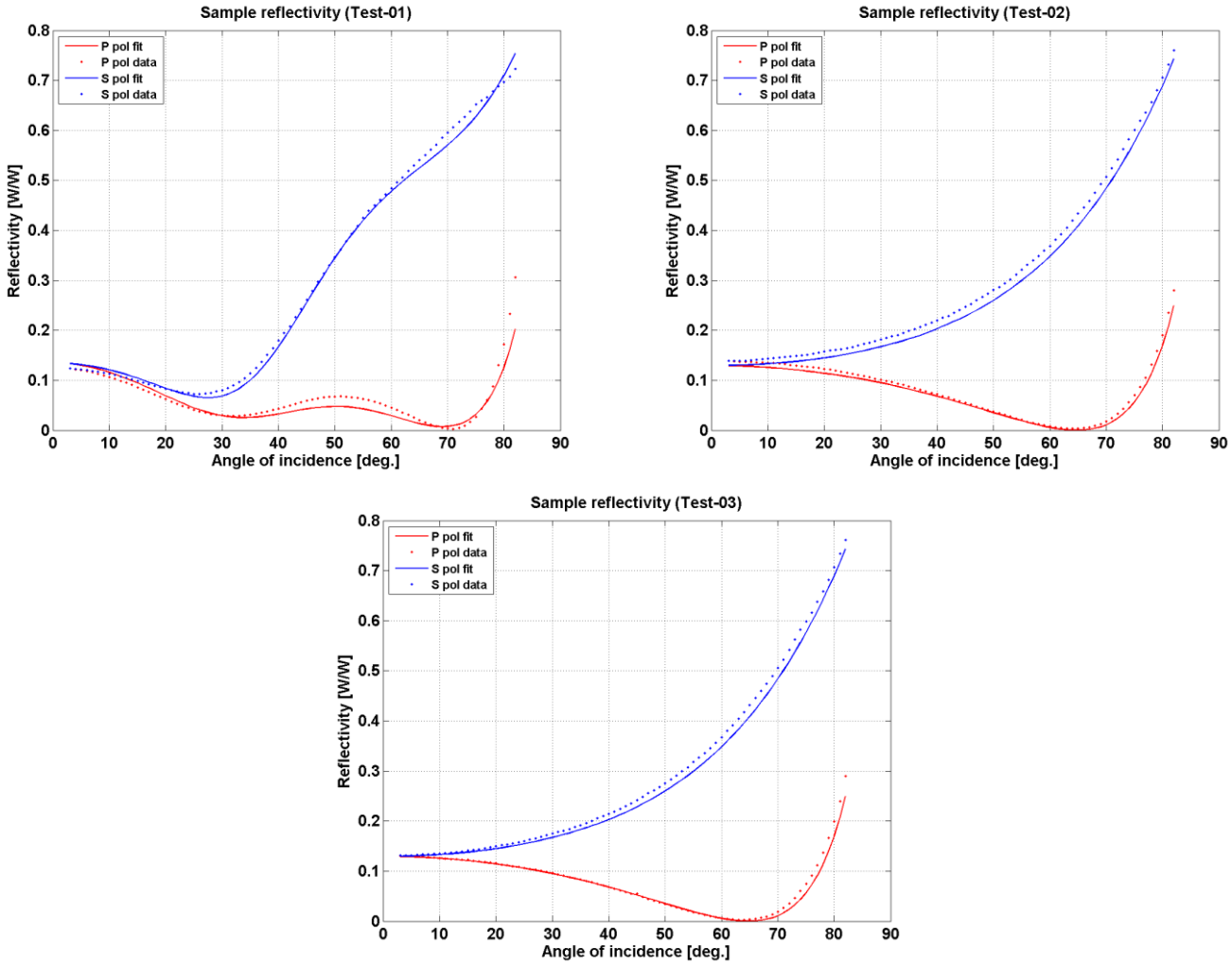

Figure 5: Global fitting for the DLC coated samples (a) of thickness 1.91µm (b) 9.76µm (c) 19.8µm

3.4. Index of refraction comparison using individual and global fitting

In this section we show the differences in the reflectivity values due to the difference in the n1 values found in global and local fitting processes for each of the three samples.

Please refer to figure 6; where P-g: Reflectivity for P-polarized incident beam for global fit;
P-l: Reflectivity for P-polarized incident beam for individual fit;
P-data: Reflectivity measured for P-polarized incident beam;
S-g: Reflectivity for S-polarized incident beam for global fit;
S-l: Reflectivity for S-polarized incident beam for individual fit;
S-data: Reflectivity measured for S-polarized incident beam;

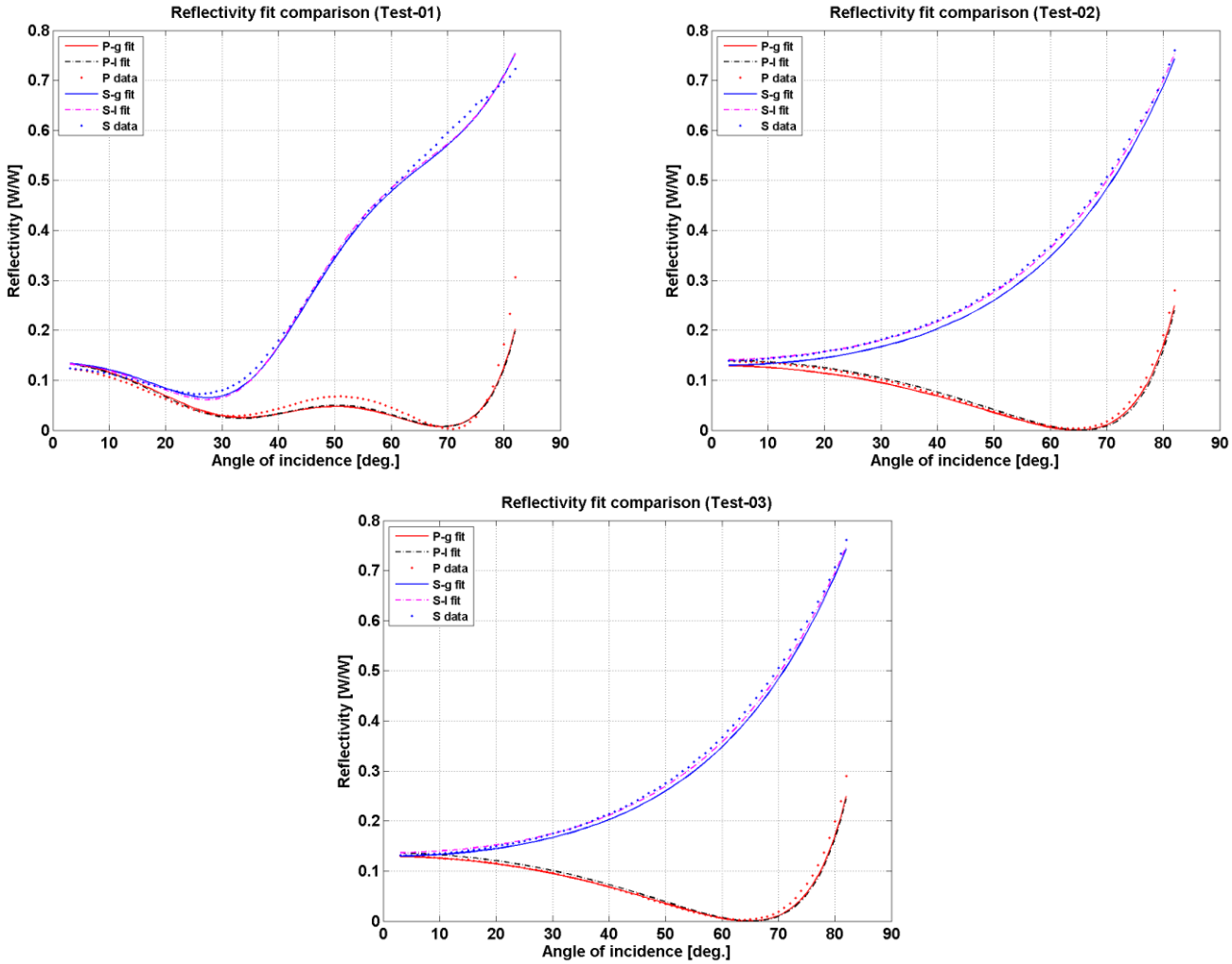

Figure 6: Comparison between local and global fitting for the DLC coated samples (a) of thickness 1.91µm (b) 9.76µm (c) 19.8µm

Table 1 provides a quick view of differences in refractive index n1 for individual and global fitting processes.

Sample	Thickness(µm)	n_1 (individual)	n_1 (global)
Test-01	1.91	2.1193 -0.0626i	2.1204 -0.0645i
Test-02	9.76	2.1985 -0.0668i	
Test-03	19.8	2.1673 -0.0658i	

Table 1: Global and local fit parameters for DLC reflectivity

3.5. Absorption

The imaginary part of the refractive index is related to absorption coefficient as

$$\alpha_{DLC} = 4\pi \frac{|Im(n_1)|}{\lambda} = 7.6 \times 10^3 cm^{-1} \quad (7)$$

When a beam of intensity I_0 illuminates the DLC layer of thickness 't', it refracts inside DLC at the boundary of n_0 and n_1. This beam is then reflected by the stainless steel substrate into the DLC. After the round trip travel inside the DLC coating a beam of intensity I_t emerges, hence we can determine the attenuated beam I_t/I_0. The residual intensity after a round trip in a 9.76µm thick DLC coating is 0.34ppm. A DLC layer of thickness 9.76µm provides enough absorption for SLC purposes (<1ppm residual intensity).

$$\frac{I_t}{I_0} = exp(\alpha_{DLC} \times 2t) \tag{8}$$

Table 2 provides the residual intensity after a round trip loss with the corresponding thickness of the respective DLC coated samples.

I_t/I_0 [ppm]	**Thickness[µm]**
5×10^{4}	1.91
0.34	9.76
8.4×10^{-8}	19.8

Table 2: The residual relative intensity after the light travels a round trip inside the DLC coated samples.

4. Total integrated scattering

The total integrated scattering of DLC coated samples were measured with the setup shown in Fig. 7. The same laser source, lenses (L1, 2), wave plates (QWP, HWP) and polarizing beam splitters (PBS1, 2) were used as in the reflection setup, but the beam is now directed towards an integrating scattering sphere (IS). The integrating sphere has five ports (Dia = 25mm), four of them located on each side of the rectangular box that shields the integrating sphere. A photo diode sensor was mounted on the fifth port located on the top of the box. The sample is mounted close to the port that is orthogonal to the illuminating beam. The sample is slightly tilted (≈ 2°- 3°) so that the specularly reflected light off the sample was sent out of the integrating sphere and dumped on a beam dump. This ensures that the measured light using a photo diode (PD) and power meter (PM) is due to only scattering. All the unwanted light was terminated with the help of beam dumps (BD1, 2 and Dumps), also the diaphragms block unwanted light around the laser beam (D1, 2, and 3). The beam size at the sample was measured as ≈ 0.25mm. An ideal diffuser with Lambertian scatter profile was used as a reference. In practice, we measured the ratio between the power P_{ref} scattered off the reference surface (scattering efficiency 100%) and the power P_{scat} scattered off the sample under investigation with the same impinging power. The measurements were performed by scanning the sample and by rotating the sample about the optical axis.

$$TIS = \frac{\langle P_{scat} \rangle}{P_{ref}} \tag{9}$$

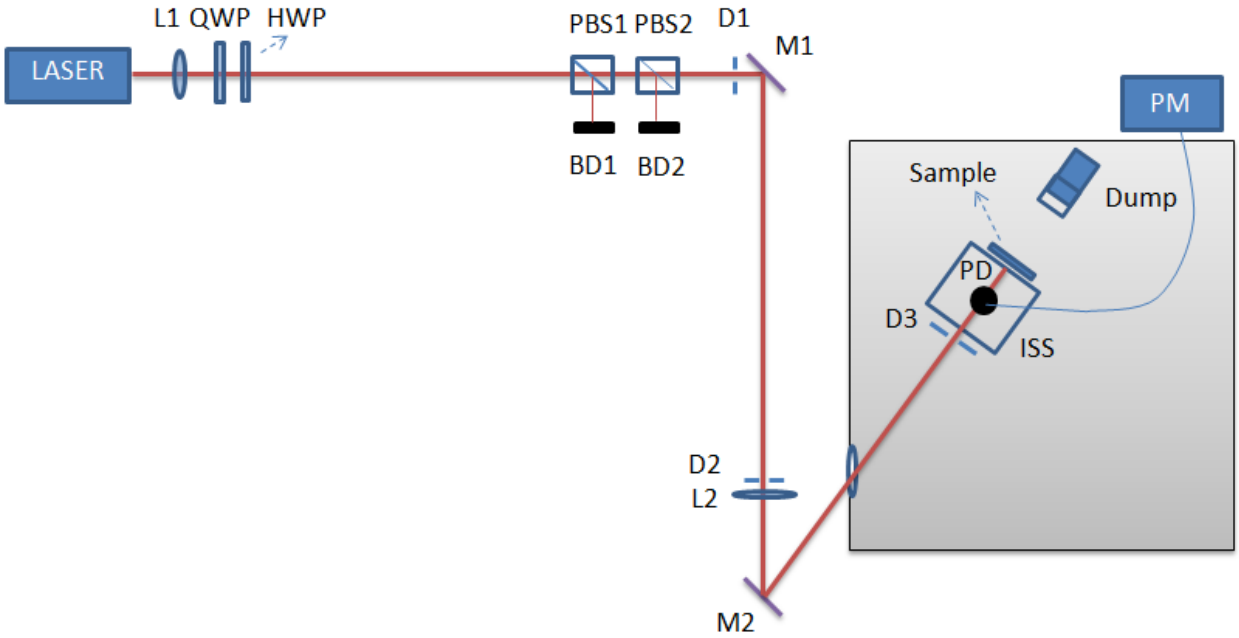

Figure 7: Total integrated scattering measurement setup

Table 3 shows the averaged TIS values for three test samples of DLC coating.

Sample	Thickness[µm]	TIS[ppm]
Test-01	1.91	700 - 1100
Test-02	9.76	1270 - 1860
Test-03	19.8	4400 - 5200

Table 3: Measured TIS at θ_{inc}~2° − 3° for the DLC coated test samples

A gradual increase of TIS value from center to the outer edges was observed. We have reported here the average TIS value of several measurements performed on the central area for each of the samples.

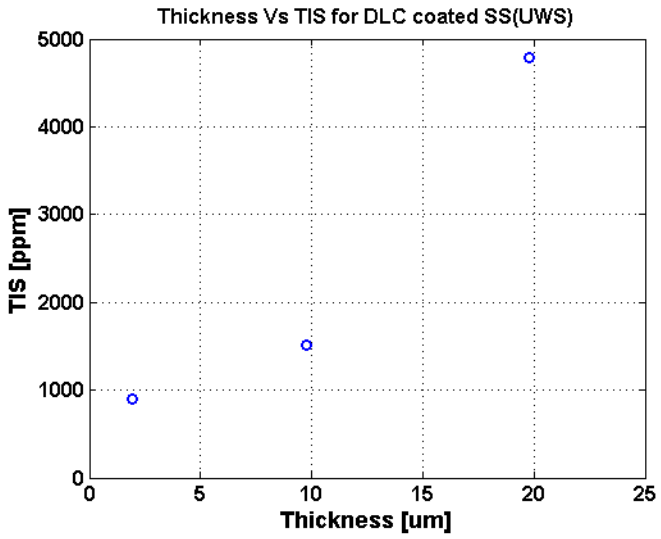

Figure 8: Total integrated scattering variation with the thickness of the DLC layers

It seems like the relationship between the thickness and TIS values of the DLC coated samples is not linear, see Figure 8. Of course more data would be needed to confirm this hypothesis.

5. In-vacuum damage threshold

A test sample (Test-02) was placed under vacuum of 10^{-5} mbar. In the above conditions the only thermal dissipation mechanisms are the thermal radiation and conduction, while convection is negligible. The sample was mounted with mechanical contacts as small as possible between the mount and sample, so that the heat dissipation was made difficult. The objective of these tests is to estimate the optical power density resistance of the DLC coated sample with environmental conditions as similar as possible to the working conditions inside the AdV interferometer. In this context, any change in the optical properties is considered as damage.

5.1. Experimental setup

The experimental setup (Figure 9) consists of a high power laser, a vacuum chamber, suitable mode matching optics and monitoring devices (temperature, camera). The Ytterbium fiber laser operates at 1075nm, so not exactly the AdV laser wavelength, but close enough for our purposes. A suitable telescope was used to focus the beam to the desired size onto the sample. The sample was placed where the beam size was ≈1.7mm (radius at $1/e^2$ intensity), then the beam power was slowly increased with the help of a half-wave plate and polarizing beam splitter combination, up to several Watts.

The intensity of the beam for the damage threshold given on this document is the mean power at $1/e^2$ send to the sample for a surface for a beam size at the same intensity, according with the fact than a Gaussian beam present a maximum peak intensity two time higher respect to the mean intensity.

$\boldsymbol{I_d = \frac{P_0 - P_r}{S}}$ is given in W/cm^2, where $\boldsymbol{P_0}$ is the input power, $\boldsymbol{P_r}$ is the non absorbed reflected power and S the area on the beam at $1/e^2$ clipping.

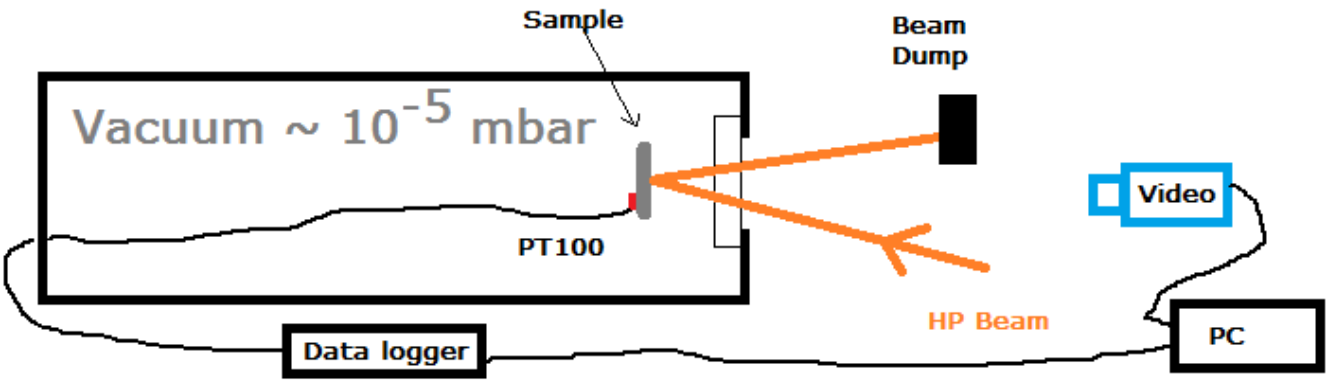

Figure 9: Experimental setup for Damage threshold measurement

In order to measure the sample temperature during the test, a PT100 thermal probe was attached to the back of the sample. A video camera was installed to monitor the heating process. The scattered pattern from the

surface of the sample was used to determine the effect of the laser beam. A good indicator about the induced damage on the sample is the modification of the diffused pattern on the spot location.

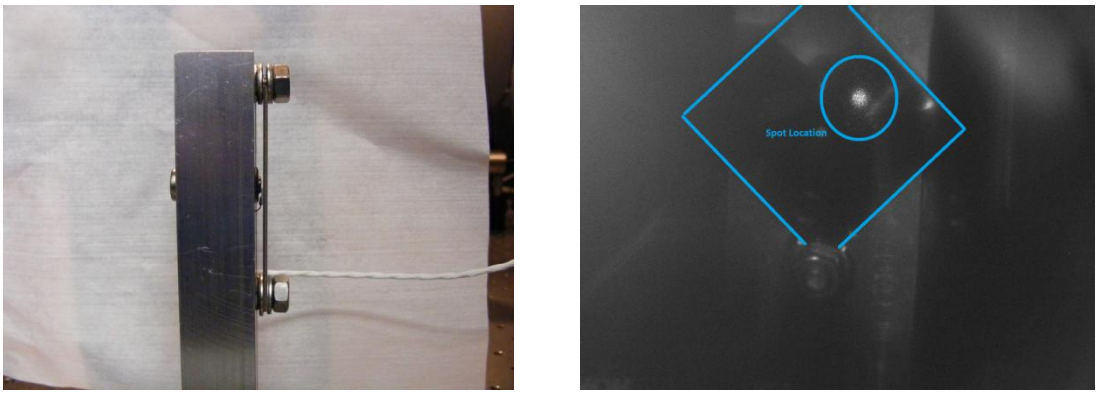

(a) **(b)**

Figure 10: (a) Sample with PT100 thermocouple mounted on the support (b) sample in the vacuum chamber with clearly visible spot location captured by a video camera

In order to monitor the temperature of the sample on the beam location, the beam is positioned on air at low power (500mW) on the position where the temperature read by the PT100 is maximum. The first test is to identify roughly the damage threshold. Figure 10 shows the sample in the vacuum chamber.

5.2. Test on 10µm DLC-coated plate

The first test had as a goal to estimate roughly the damage threshold of the material. The beam was pointed on the centre of the sample and the input optical power increased by coarse steps. In order to reproduce our real working conditions, we waited several minutes between two steps for temperature stabilization.

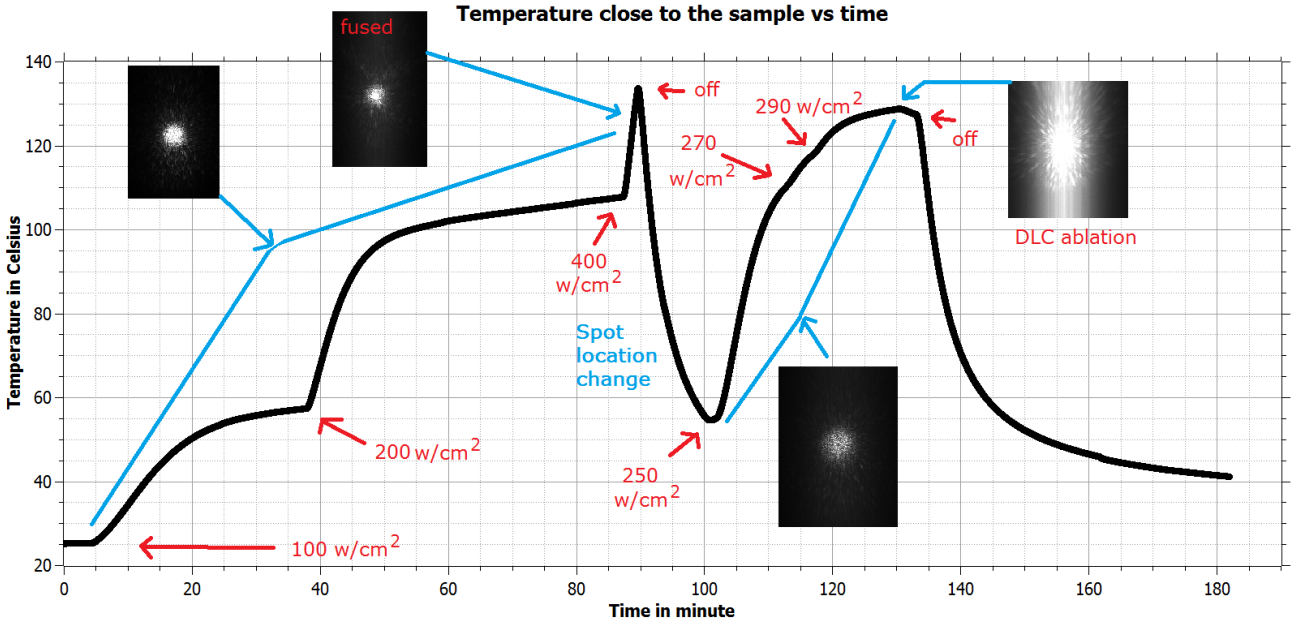

Figure 11: First tests for Damage threshold estimation for Test-02 (10um thick DLC) sample

Unfortunately for the first test, the temperature probe moved with respect to the initial position, so the temperature given on the plot is not the temperature close to the beam location.

The first impact after the first shot inspected by eyes trough the viewport of the vacuum chamber was really similar to the impact shows on figure 15. This damage correspond to the first picture noted “fused” on the Figure 11. After changing the beam impact location, the sample was shone again in order to estimate the damage threshold more accurately. The second shot induced a damage for **290 W/cm^2**, the diffusion pattern was really different respect to the first one (see and the second part of figure 11 were it is mentioned DLC ablation). In particular it was much brighter, meaning more scattered light.
After inspection of the sample, it was possible to see the ablation area bigger than the first one. Furthermore, the first damaged area suffered some changes after this second run, even though the two impact points are several millimetres away from each other. Figure 12 shows the first and the second impact once out of the chamber.

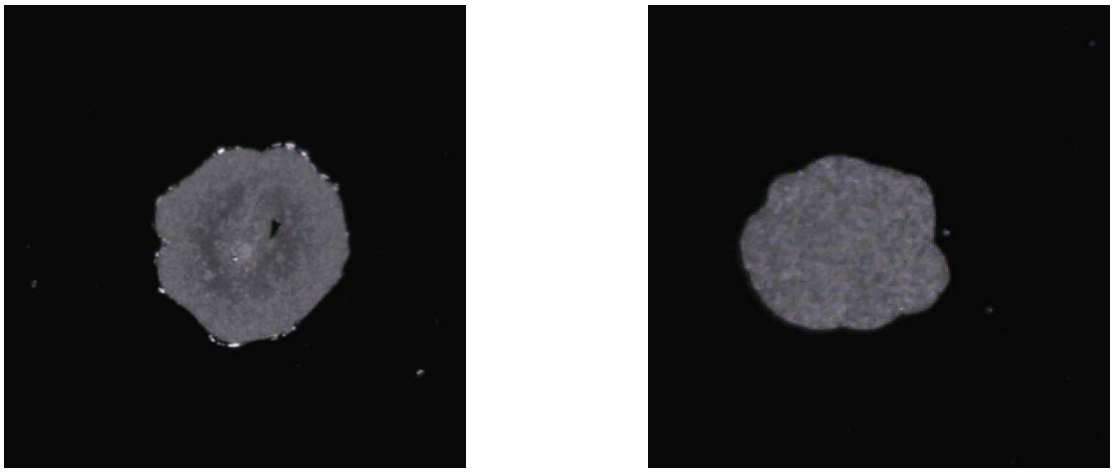

First impact (after second impact) **Second impact**

Figure 12: (a) Laser induced damage of the Test-02 sample on first impact (b) on second impact

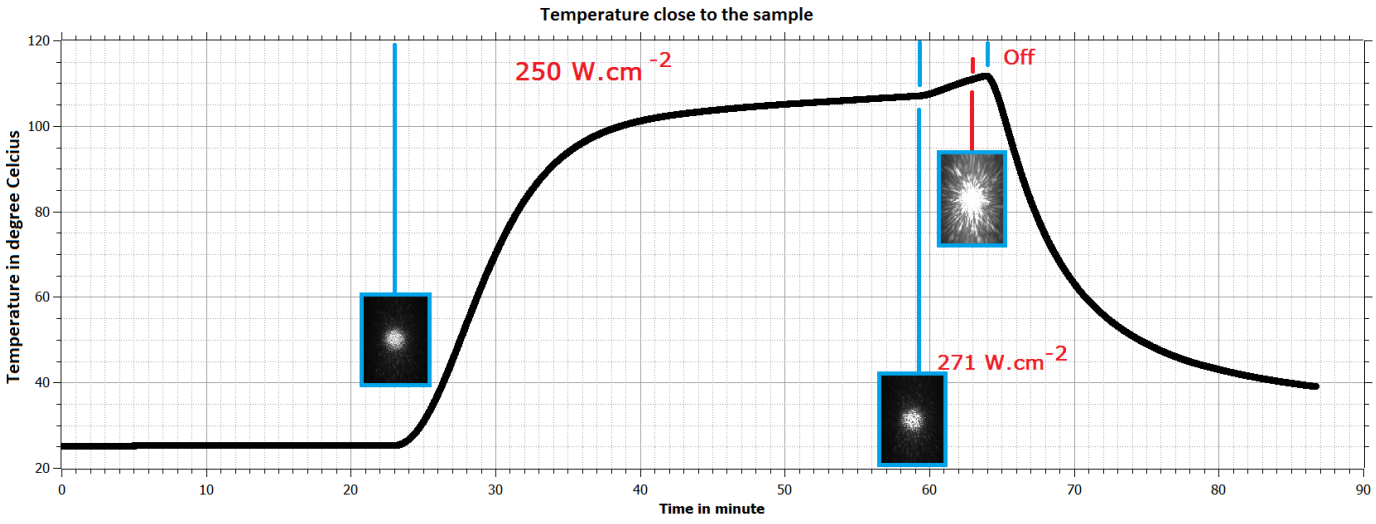

Figure 13: Measurement of damage threshold for Test-02 (10um thick DLC) sample. At time 63min, increase of brightness shows that damage has occurred.

The beam size was changed once more for a third measurement and the damage threshold was found to be between **0.25KW/cm^2** and **0.27 KW/cm^2**. The third damaged area was really similar to the second one and this time no further changes occurred to the two previous impacts, as shown on figure 13.

5.3. Test on 20µm DLC coating plate

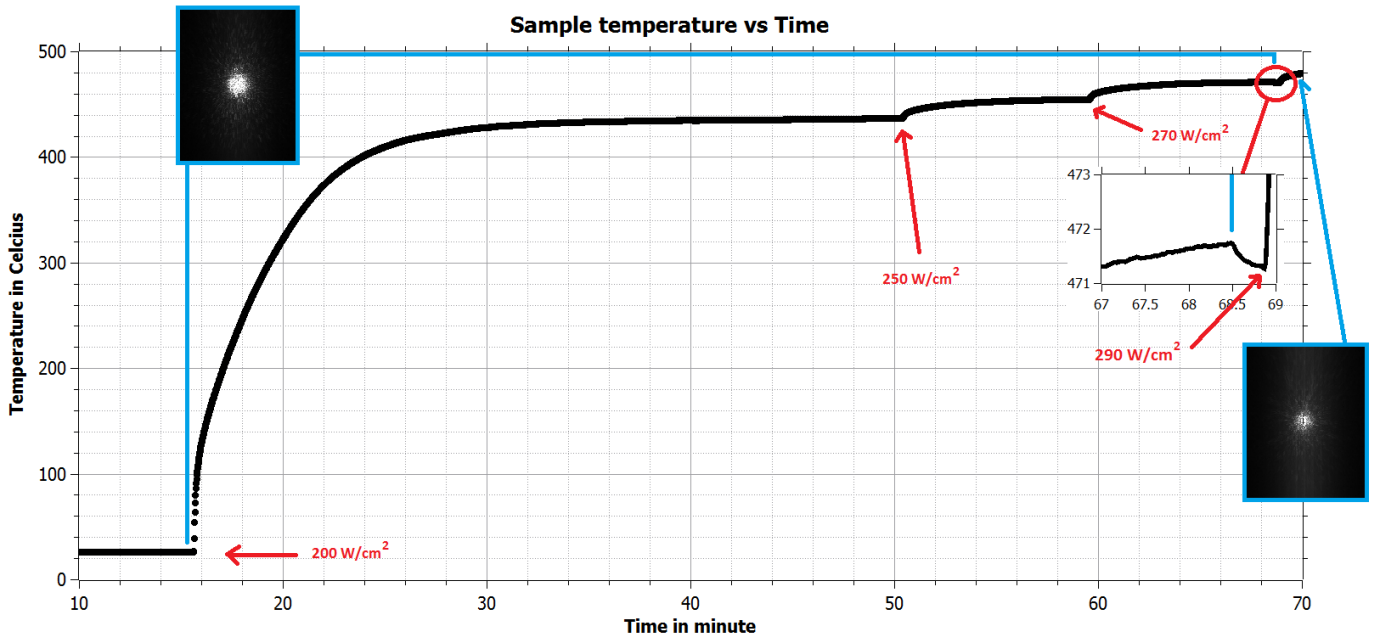

Figure 14: Laser induced damage threshold estimation for Test-03 (20um thick DLC) sample

It was reproduced the same tests on the 20µm thick DLC sample and this time, the temperature probe was fixed strong enough to keep the well position : behind the spot location.
As expected, the induced damage threshold is the same than for the 10um sample.
Due to the absence of convection in vacuum, the temperature of the sample reaches **480 °C** on the spot location.

The Figure 15 shows the DLC ablation of the sample.

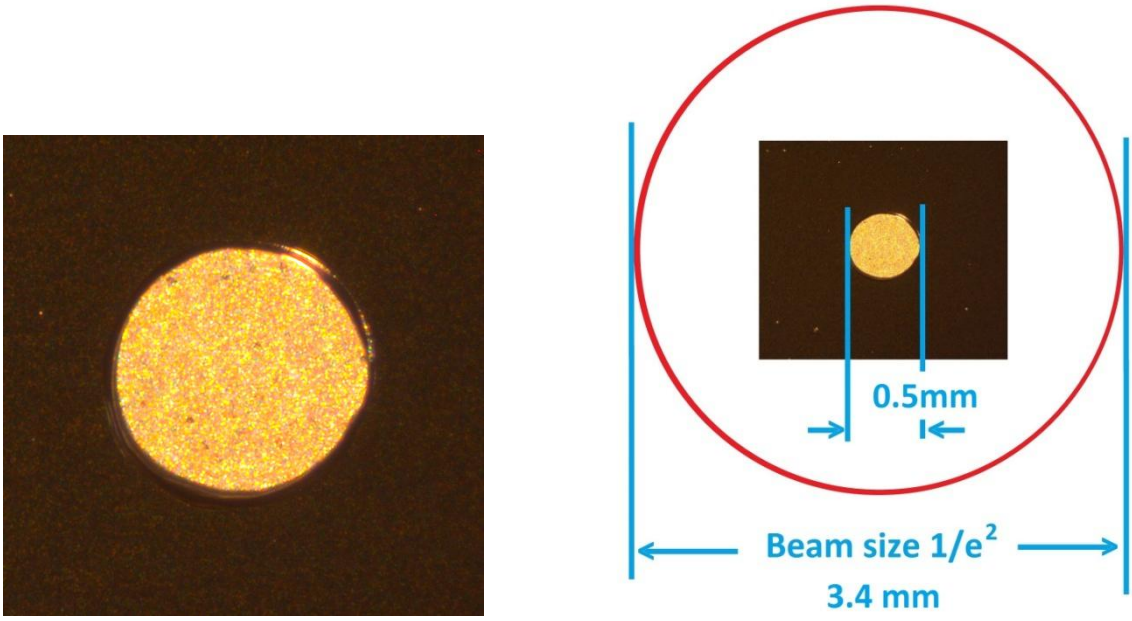

(a) **(b)**

Figure 15: Induced damage of the Test-03 sample (a) impact (b) on scale with the beam size.

6. Conclusion

We have measured the reflectivity of the DLC layers coated on stainless-steel substrates for both s and p polarized illuminating beams. The reflectivity measurements were fitted using minimum residual error function individually for each of the test samples and also altogether. From the global curve fit we found the refractive index of the DLC as n_1= 2.12 -0.064i, which is roughly in agreement with the reported values for other DLC measurements n_1= 2.4 -0.04i [2] and n_1= 2.2 - 0.05i [3]. The TIS value for thin DLC layer of thickness ~1.9µm is 900ppm and for ~19.8µm layer is of the order of 4800ppm. When compared to the TIS of the DLC reported in ref. 2 (for a layer of thickness ~1µm is 320ppm and for a layer ~15µm is 5400 – 6900ppm) the TIS value for thin DLC layers is rather larger.

The damage threshold induced by a Gaussian laser beam at 1075nm is up to **0.25KW/cm^2** for a long term exposure under vacuum.

7. References

[1] The VIRGO collaboration, “Advanced Virgo Technical Design Report”, VIR-0128A-12 https://tds.ego-gw.it/ql/?c=8940

[2] A. Chiummo, "AdV SLC: Characterization of diamond-like carbon for coating baffles and beam dumps in AdV", VIR-0127A-13

[3] R. Takahashi, Y. Saito, Y. Sato, T. Kubo, T. Tomaru, M. Tokunari, T. Sumiya, K. Takasugi, Y. Naito, “Application of diamond-like Carbon (DLC) coatings for gravitational wave detectors”, Vacuum 73 (2004) 145-148